Knockdown of lncRNA LINC01234 suppresses the tumorigenesis of liver cancer via sponging miR-513a-5p

Wen Xu
East China University of Science and Technology
Kesang Li
University of Chinese Academy of Science
Changfeng Song
East China University of Science and Technology
Xiaotong Wang
East China University of Science and Technology
Yueqi Li
East China University of Science and Technology
Xue Bai
East China University of Science and Technology
Xin Liang
East China University of Science and Technology
Wanli Deng
Shuguang Hospital
Junqing Wang
Ruijin Hospital
Jianwen Liu (jianwen_ecust@126.com)
East China University of Science and Technology

Research

Keywords: liver cancer, LINC01234, USP4, miR-513a-5p

Posted Date: March 25th, 2020

DOI: https://doi.org/10.21203/rs.3.rs-19098/v1

Version of Record: A version of this preprint was published at Frontiers in Oncology on October 16th, 2020. See the published version at https://doi.org/10.3389/fonc.2020.571565.

Abstract

Background Liver cancer is a frequent malignancy with poor prognosis. It has been reported that many lncRNAs could regulate the progression of liver cancer. To identify potential therapeutic targets for liver cancer, we conducted bioinformatics analysis of lncRNAs in tumor tissues and adjacent normal tissues.

Methods The differential expression of lncRNAs between liver cancer tissues and adjacent normal tissues were examined by bioinformatics analysis. Cell proliferation was tested by CCK-8. Cell apoptosis in liver cancer was detected by flow cytometry. Gene and protein expression in liver cancer cells were measured by q-PCR and Western-blot, respectively. Xenograft tumor model was established to verify the function of LNC01234 on liver cancer in vivo.

Results LNC01234 was found to be notably upregulated in liver cancer tissues. In addition, knockdown of LNC01234 significantly inhibited the proliferation, invasion and induced the apoptosis of liver cancer cells. Meanwhile, miR-513a-5p was a downstream target of LNC01234 and USP4 was a direct target of miR-513a-5p. Moreover, downregulation of LNC01234 inhibited the tumorigenesis of liver cancer via inactivating TGF-β signaling.

Conclusion Downregulation of LNC01234 could inhibit the progression of liver cancer, which may serve as a potential novel target for treatment of liver cancer.

Introduction

Liver cancer is a common malignant tumor, with a 15–17% 5-year survival rate (1, 2). The prognosis of patients with liver cancer is poor due to the high frequency of postoperative recurrence and metastasis (3). Surgery is still the main treatment strategy. However, liver cancer patients are usually diagnosed at advanced stages, so they often miss the optimal opportunity for surgical resection (4). Furthermore, liver cancer is highly resistant to conventional chemotherapy and radiation therapy (5, 6). Currently, clinicopathologic prognostic factors include TNM stage, tumor size, microvascular invasion, tumor rupture, underlying cirrhosis, and multi-focality (7). In addition to these traditional clinical prognostic factors, genetic biomarkers are novel indicators of liver cancer diagnosis and prognosis (8). Molecular biomarkers can help predict patient prognosis (9), but there is still a lack of biomarkers for clinical management of liver cancer. Therefore, it is necessary to adopt a comprehensive approach to identify novel tumor biomarkers and explore potential molecular mechanisms.

LncRNAs are endogenous RNAs with a covalently closed cyclic structure (10). Intracellular lncRNAs with competing endogenous RNAs (ceRNAs) activity may act as miRNA sponges through binding miRNAs with MREs, which greatly inhibit the activity of miRNA and result in upregulating the expressions of genes targeted by miRNA (11). Therefore, lncRNAs have been considered important biological regulators for exploring the molecular mechanisms of multiple diseases and identifying therapeutic targets.

Previous reports have indicated the importance of lncRNAs in modulating cancer-related signaling pathways (12, 13). Moreover, lncRNAs may be related with types of malignant tumors and serve as key factors for tumorigenesis of many cancers (14). However, the function of lncRNAs during the progression of liver cancer remains to be further explored. In this research, we used a systemic bioinformatics analysis to identify lncRNAs that are essential for the biological processes of liver cancer, which may supply potential targets for the development of novel therapeutic strategies against liver cancer.

Material And Methods

Cell culture

Liver cancer cell lines (HepG2 and Huh-7) and 293T cells were obtained from the American Type Culture Collection (ATCC, Manassas, VA, USA) and cultured in Dulbecco's Modified Eagle's Medium (DMEM, Thermo Fisher Scientific, Waltham, MA, USA) with 10% FBS (Thermo Fischer Scientific), 1% penicillin and streptomycin (Thermo Fisher Scientific) at 37°C, 5% CO_2.

Bioinformatics analysis

One dataset (GSE113850) which contain the gene expression data liver cancer tissue and adjacent normal tissue (controls) were obtained from GEO database (https://www.ncbi.nlm.nih.gov/geo/). The relation between lncRNA/USP4 and tumor stage of liver cancer was analyzed. The survival curve was calculated using the Cancer Genome Atlas (TCGA).

Quantitative real time polymerase chain reaction (qRT-PCR)

Total RNA was extracted from liver cancer cell lines using TRIzol reagent (TaKaRa, Tokyo, Japan) according to the manufacturer's protocol. cDNA was synthesized using the reverse transcription kit (TaKaRa, Ver.3.0) according to the manufacturer's protocol. Real-Time qPCRs were performed in triplicate under the following protocol: 2 minutes at 94°C, followed by 35 cycles (30 s at 94°C and 45 s at 55°C). The primer for LINC01234, miR-513a-5p, β-actin and U6 were obtained from GenePharma (Shanghai, China). LINC01234: forward, 5'- CAGGACCTTCTGTGGGACTC-3' and reverse 5'-TCCAAAACTCCCCTTTCCCA-3'. MiR-513a-5p: forward, 5'- TGCGCTCAGCAAACATTTATTG-3' and reverse 5'- CCAGTGCAGGGTCCGAGGTATT-3'. β-actin: forward, 5'-AGCGAGCATCCCCCAAAGTT-3' and reverse 5'-GGGCACGAAGGCTCATCATT-3'. U6: forward, 5'-CGCTTCGGCAGCACATATAC-3' and reverse 5'-AAATATGGAACGCTTCACGA-3'. The relative fold changes were calculated using the $2^{-\Delta\Delta Ct}$ method by the formula: $2^{-(\text{sample } \Delta Ct - \text{control } \Delta Ct)}$, where ΔCt is the difference between the amplification fluorescent thresholds of the gene of interest and the internal reference gene (U6 or β-actin) used for normalization.

Cell transfection

Lentiviral expressing short-hairpin RNA (shRNA1 or shRNA2) directed target LINC01234 and one nontargeting sequence (negative control) were obtained from Hanbio Biotechnology Co., Ltd (Shanghai,

China). Next, LINC01234 shRNA1 or shRNA2 was packaged into lentiviruses. Then the lentiviral vector DNAs were then transfected into 293T cells including lenti-LINC01234 shRNAs and negative control (NC). After transfection, the cells were incubated at 32˚C, and then the supernatant was collected. After that, supernatants of two LINC01234 shRNAs and negative control were filtered into particles. Finally, all liver cancer cells were infected with lentiviral particles according to the manufactures' protocol. After 48 h of incubation, stable liver cancer cells were then selected by puromycin (2.5 μg/mL, Sigma Aldrich, St. Louis, MO, USA). Green fluorescence and qRT-PCR were used to verify the efficiency of transfection.

For miR-513a-5p transfection, liver cancer cells were transfected with miR-513a-5p agomir, miR-513a-5p antagomir or NC by Lipofectamine 2000 according to the previous reference (15). MiR-513a-5p agomir, miR-513a-5p antagomir and negative control RNAs were purchased from GenePharma (Shanghai, China). The efficiency of transfection was detected by q-PCR.

CCK-8 assay

Liver cancer cells were seeded in 96-well plates (5×10^3 per well) overnight. Then, cells were treated with negative control (NC) or LINC01234 shRNA1 for 0, 24, 48 and 72 h, respectively. 10 μl CCK-8 reagents were added to each well and further incubated for 2 h at 37°C. Finally, the absorbance of liver cancer cells was measured at 450 nm using a microplate reader (Thermo Fisher Scientific).

Cell apoptosis analysis

Liver cancer cells were trypsinized, washed with phosphate buffered saline and resuspended in Annexin V Binding Buffer, followed by staining with 5 μl FITC and 5 μl propidium (PI) in the system for 15 min. Cells were analyzed using flow cytometer (BD, Franklin Lake, NJ, USA) to test the cell apoptosis rate.

Cell invasion assay

For cell invasion analysis, transwell assay was performed in this study. The upper chamber is pre-treated with 100 μl of Matrigel. Huh7 cells were seeded into the upper chamber in media with 1% FBS, and the density was adjusted to about 1.0×10^6 cells per chamber. RPMI1640 medium with 10% FBS was added in the lower chamber. After 24 h of incubation at 37°C, the transwell chamber was rinsed twice with PBS (5 min per time), fixed by 5% glutaraldehyde at 4°C and stained with 0.1% crystal violet for 30 minutes. The transwell chamber was washed twice with PBS and then observed under a microscope. The number of cells invading the Matrigel was regarded to be a reflection of the invasion ability.

Dual luciferase reporter assay

The partial squences of LINC01234 and 3'-UTR of USP4 containing the putative binding sites of miR-513a-5p were synthetized and obtained from Sangon Biotech (Shanghai, China), then were cloned into the pmirGLO Dual-Luciferase miRNA Target Expression Vectors (Promega, Madison, WI, USA) to construct wild-type reporter vectors LINC01234 (WT) and USP4 (WT), respectively. The mutant LINC01234 sequences and 3'-UTR of USP4 sequences containing the putative binding sites of miR-513a-5p were

performed by Q5 Site-Directed Mutagenesis Kit (New England Biolabs, Ipswich, MA, USA) and then cloned into pmirGLO vectors respectively, to construct mutant-type reporter vectors LINC01234 (MUT) and USP4 (MUT). The LINC01234 (WT) or LINC01234 (MUT) was transfected into 293T cells together with control, vector-control (NC) or miR-513a-5p agomir using Lipofectamine 2000 (Thermo Fisher Scientific) according to the manufacturer's instructions. Similarly, the USP4 (WT) or USP4 (MUT) was transfected into 293T cells together with control, vector-control (NC) or miR-513a-5p agomir. The relative luciferase activity was analyzed by the Dual-Glo Luciferase Assay System (Promega).

RNA pull-down

For the RNA pulldown assay, the Biotin RNA Labeling Mix (Roche, Basel, Switzerland) was used to transcribe and label probe-control or probe-LINC01234 from LINC01234 shRNA lenti vector *in vitro*. An RNA structure buffer (Thermo, MA, USA) was used to induce secondary structure formation from the biotin-labeled RNAs. Streptavidin beads (Thermo) were washed three times with 500 μL of RNA immunoprecipitation wash buffer (Thermo) and then added to the biotinylated RNAs at 4°C overnight. The overnight mixture was separated by a magnetic field so that streptavidin bead-RNA complexes could be obtained. Then, lysates of liver cancer cells were added to the complexes and incubated on a rotator at room temperature for one hour. The incubated mixture was again separated with a magnetic field so that streptavidin bead-RNA-protein complexes could be obtained.

Wound healing assay

Huh-7 cells were plated into a 24-well Cell Culture Cluster, and were allowed to grow to 80-90% confluence. Then, cells were underlined perpendicular to the cell culture plate with a small pipette head. After washing with PBS 3 times, serum-free medium was used for further culture, and the scratch widths at 0 and 48 h were recorded under an optical microscope. The experiment was repeated 3 times.

Immunofluorescence

Liver cancer cells or tumor tissues of mice were prefixed in 4% paraform for 10 min, and fixed in pre-cold methanol for another 10 min. Next, cells were incubated with primary antibodies overnight at 4°C: anti-Ki67 (Abcam; 1:1000), anti-Smad4 (Abcam; 1:1000) and DAPI (Abcam; 1:1000). Goat anti-rabbit IgG antibody (Abcam; 1:5000) was used as the secondary antibody. The samples were visualized by fluorescence microscope (Olympus CX23, Tokyo, Japan) immediately.

Western-blot detection

Total protein was isolated from cell lysates or tumor tissues by using RIPA buffer, and quantified by BCA protein assay kit (Beyotime, Shanghai, China). Proteins were resolved on 10% SDS-PAGE, and then transferred to PVDF (Bio-Rad) membranes. After blocking, the membranes were incubated with primary antibodies at 4°C overnight, then incubated with secondary anti-rabbit antibody (Abcam; 1:5000) at room temperature for 1 h. Membranes were scanned by using an Odyssey Imaging System and analyzed with Odyssey v2.0 software (LICOR Biosciences, Lincoln, NE, USA). Then, the primary antibodies used in this

study as follows: anti-E-cadherin (Abcam, Cambridge, MA, USA; 1:1000), anti-vimentin (Abcam; 1:1000), anti-α-SMA (Abcam; 1:1000), anti-smad2 (Abcam; 1:1000), anti-smad3 (Abcam; 1:1000), anti-USP4 (Abcam; 1:1000), anti-cleaved caspase 3 (Abcam; 1:1000), anti-Akt (Abcam; 1:1000), anti-ERK (Abcam; 1:1000) and anti-β-actin (Abcam; 1:1000). β-actin was used as an internal control.

In vivo study

18 BALB/c nude mice (6-8 weeks old) were purchased from Vital River (Beijing, China). The mice were housed within a dedicated SPF facility. Huh7 stable expressed LINC01234 shRNA1 cells were transplanted subcutaneously in each mouse according to the previous reference (16). The tumor volume was measured weekly according to the reference (17). At the end of the experiments, mice were sacrificed and the tumors were collected and weighted. The expression of p-smad2 and p-smad3 were detected by immunohistochemistry (IHC) staining as previously reported (18). All *in vivo* experiments were performed in accordance with National Institutes of Health guide for the care and use of laboratory animals, following a protocol approved by the Ethics Committees of East China University of Science and Technology.

TUNEL staining

Apoptosis was also determined by the TUNEL assay according to the manufacturer's instructions. Briefly, paraffin sections were washed, permeabilized, and then incubated with 50 μl TUNEL reaction mixtures in a wet box for 60 min at 37°C in the dark. For signal conversion, slides were incubated with 50 μl of peroxidase (POD) for 30 min at 37°C, rinsed with PBS, and then incubated with 50 μl diaminobenzidine (DAB) substrate solution for 10 min at 25°C. Finally, the expression of apoptotic cells was observed under an optical microscope.

Statistical analysis

Each group were performed at least three independent experiments and all data were expressed as the mean ± standard deviation (SD). Differences were analyzed using Student’s t-test (only 2 groups) or one-way analysis of variance (ANOVA) followed by Tukey’s test (more than 2 groups, Graphpad Prism7). $P<0.05$ was considered to indicate a statistically significant difference.

Results

Differentially expressed lncRNAs in liver cancer

To detect differentially expressed lncRNAs in hepatic carcinoma, we performed a bioinformatics analysis. As indicated in Figure 1A, lncRNAs differentially expressed as compared to normal tissues in the GSE113850 dataset were presented as volcano plots. In addition, differentially expressed lncRNAs among normal and tumor tissues were also presented in TCGA (Figure 1B). Overlap among GSE113850 dataset was illustrated by the Venn diagram in Figure 1C. Among the differentially expressed lncRNAs,

167 were upregulated, while 59 were downregulated in GSE113850. Moreover, LINC01234 was closely correlated with the tumorigenesis of hepatic carcinoma. Thus, LINC01234 was selected for further study.

The expression of LINC01234 was significantly upregulated in liver cancer tissues, compared to normal tissues (Figure 1D). In addition, LINC01234 expression in tissues of advanced liver cancer was obviously enhanced, compared to stage I/II liver cancer tissues (Figure 1E). Besides, the result of overall/disease free survival analysis showed that LINC01234 was closely associated with poor survival of hepatic carcinoma (Figure 1F and 1G). These results suggested that LINC01234 was upregulated in hepatic carcinoma.

LINC01234 silencing significantly decreased the proliferation of liver cancer cells

In order to detect the efficiency of cell transfection, green fluorescence was used. As showed in Figure 2A and 2B, the results indicated that LINC01234 shRNA1 and shRNA2 were stably transfected into liver cancer cells. In addition, the results were further verified by q-PCR (Figure 2C). Since LINC01234 shRNA1 exhibited better transfection efficiency, it was therefore used in subsequent experiments. Next, CCK-8 and Ki-67 staining were performed to test the cell proliferation of hepatic carcinoma. As demonstrated in Figure 2D-2G, the proliferation of Huh-7 and HepG2 cells were significantly inhibited by downregulation of LINC01234. Meanwhile, Huh-7 cells were more sensitive to LINC01234 shRNA1 than HepG2 cells, Huh-7 cells were used in the following experiments. Taken together, LINC01234 silencing significantly decreased the proliferation of liver cancer cells.

LINC01234 sponged miR-513a-5p

For the purpose of exploring the mechanism by which LINC01234 mediated the progression of liver cancer, Starbase (http://starbase.sysu.edu.cn/) was performed. As showed in Figure 3A, miR-513a-5p might be the downstream target of LINC01234. In addition, miR-513a-5p agomir/antagomir was stably transfected into Huh-7 cells (Figure 3B). Meanwhile, the result of dual luciferase report assay and RNA pull-down confirmed that LINC01234 could bind to miR-513a-5p (Figure 3C and 3D). To find the target of miR-513a-5p, targetscan (http://www.targetscan.org/vert_71/) and dual luciferase were used. As revealed in Figure 3E and 3F, miR-513a-5p directly targeted USP4. Additionally, the expression of USP4 in tissues of hepatic carcinoma was greatly increased (Figure 3G). Meanwhile, USP4 was more closely correlated with advanced liver cancer (Figure 3H). Altogether, LINC01234 could bind to miR-513a-5p.

Knockdown of LINC01234 significantly suppressed the progression of hepatic carcinoma *in vitro*

Then, flow cytometry was performed to detect the cell apoptosis. As revealed in Figure 4A, downregulation of LINC01234 notably induced the apoptosis of Huh-7 cells. In addition, the data of wound healing and invasion assay indicated that knockdown of LINC01234 greatly inhibited the migration and invasion of liver cancer cells (Figure 4B and 4C). Furthermore, western blot was used to detect the expressions of EMT-related proteins in Huh-7 cells. The results showed that the expression of E-cadherin in Huh-7 cells was significantly upregulated by LINC01234 shRNA1. In contrast, knockdown of

LINC01234 greatly decreased the expression of vimentin and α-SMA in liver cancer cells (Figure 4D). To sum up, knockdown of LINC01234 significantly suppressed the progression of hepatic carcinoma *in vitro*.

Downregulation of LINC01234 notably inhibited the tumorigenesis of hepatic carcinoma via mediation of miR-513a-5p/USP4/TGF-β1 axis

In order to investigate the protein expressions in liver cancer cells, western blot was used. As indicated in Figure 5A and 5B, the expressions of USP4, p-Smad2 and p-Smad3 in Huh-7 cells were significantly downregulated in the presence of LINC01234 shRNA1, which were partially rescued by miR-513a-5p antagomir. In addition, the expression of Smad4 in cytoplasm of Huh-7 cells was significantly decreased by downregulation of LINC01234. However, miR-513a-5p antagomir notably suppressed the inhibitory effect of LINC01234 shRNA on Smad4 expression (Figure 5C). Moreover, LINC01234 shRNA1 greatly suppressed the expressions of p-Akt and p-ERK in Huh-7 cells. In contrast, cleaved caspase 3 in Huh-7 cells was activated in the presence of LINC01234 downregulation. However, downregulation of miR-513a-5p partially reversed the effect of LINC01234 shRNA1 on these proteins (Figure 5D and 5E). In summary, downregulation of LINC01234 notably inhibited the tumorigenesis of hepatic carcinoma via mediation of miR-513a-5p/USP4/TGF-β1 axis.

Knockdown of LINC01234 notably attenuated the symptom of hepatic carcinoma *in vivo* through suppression of TGF-β signaling

Finally, to detect the effect of LINC01234 on liver cancer *in vivo*, xenograft mice model was established. As showed in Figure 6A and 6B, tumor sizes of mice were significantly decreased by downregulation of LINC01234. Similarly, knockdown of LINC01234 notably downregulated the tumor weights of mice (Figure 6C). Meanwhile, the expression of LINC01234 in tissues of mice was greatly inhibited by LINC01234 knockdown (Figure 6D). Furthermore, the data of Ki-67 and TUNEL staining demonstrated that tumor growth of mice was obviously suppressed in the presence of LINC01234 downregulation (Figure 6E-6H). Consistently, p-Smad2 and p-Smad3 in tumor tissues of mice were notably inactivated by LINC01234 silencing (Figure 6I and 6J). Altogether, knockdown of LINC01234 notably attenuated the symptom of hepatic carcinoma *in vivo*.

Discussion

LncRNAs are a group of noncoding RNAs widely distributed in humans (19) which are different from linear noncoding RNAs such as miRNAs. It has been reported that lncRNAs may mediate upregulation or downregulation of gene expression and, despite being classified as noncoding, may also encode proteins (20). Moreover, lncRNAs are stable and widely expressed in many tumor tissues (21, 22). These backgrounds suggest the possibility that lncRNAs may be involved in paracrine signaling or cell-to-cell crosstalk. Our findings indicate that LINC01234 downregulation could suppress hepatic carcinoma cell proliferation and induce apoptosis, which is consistent with earlier reports indicating that lncRNAs regulate the progression of liver cancer (23, 24). These findings suggest that LINC01234 likely acts to promote tumorigenesis of liver cancer, particularly during the advanced stages of the disease. In addition,

we firstly found the function of LINC01234 in hepatic carcinoma. This may make LINC01234 an important biomarker for diagnosis of liver cancer.

MiRNAs are known to play important roles in the progression of multiple diseases, including hepatic carcinoma (25, 26). We found that a miR-513a-5p antagomir partially reversed the inhibitory effect of LINC01234 knockdown on liver cancer. Yang L et al reported that miR-513a-5p induces downregulation of retinoblastoma cells proliferation and induce apoptosis (27). Our findings suggested miR-513a-5p was also a key regulator of liver cancer progression. In addition, Zhu Y et al demonstrated that MRVI1-AS1 enhances nasopharyngeal cancer malignancy by sponging miR-513a-5p (28). These results are similar to our present findings, indicating that LINC01234 knockdown suppresses the tumorigenesis of hepatic carcinoma by sponging miR-513a-5p. Otherwise, a previous report indicated that LINC01234 silencing could exert an anti-oncogenic effect in esophageal cancer cells through sponging miR-193a-5p (29). This difference may result from the different tumor type.

It was recently suggested that USP4 plays a key role in multiple malignant tumors (30, 31). In addition, USP4 reportedly mediates cell proliferation, survival and metastasis (32, 33). Our findings firstly indicated that USP4 is a direct target of miR-513a-5p. It has been previously confirmed that USP4 could act as a tumor promoter in liver cancer (34). These results further implicate USP4 in the development of liver cancer; indeed, it suggests USP4 a key promoter in the occurrence of liver cancer. Moreover, Jiang W et al indicated that miR-148a dysregulation could discriminate poor prognosis of hepatocellular carcinoma in association with USP4 overexpression (35). Our result was consistent to this previous study, confirming that LINC01234 could mediate the progression of liver cancer via indirectly targeting USP4.

TGF-β signaling plays a key role in various kinds of diseases, including malignant tumors (36, 37). It has been reported that TGF-β can activate Smad2 and Smad3 (38). Moreover, multiple studies have found that Smad4 loss on its own does not initiate tumor formation, but can promote fibrosis initiated by other genes, such as KRAS activation in pancreatic duct adenocarcinoma and APC inactivation in renal diseases (39). In this study, we found that LINC01234 knockdown downregulated the expression of p-Smad2, p-Smad3 in liver cancer cells. In addition, LINC01234 silencing also increased the expression of Smad4 in Cytoplasma of Huh-7 cells. Based on these data, the mechanism underlying the anti-tumor effects of LINC01234 knockdown was associated with the inactivation of TGF-β signaling pathway. According to Zhang J et al, USP4 inhibition can lead to inactivation of TGF-β signaling pathway (33). Our current research was consistent to this data, suggesting that LINC01234 could modulate the tumorigenesis of liver cancer via mediation of USP4/TGF-β axis.

Besides, we also found that the expression of E-cadherin, α-SMA and vimentin were notably regulated in Huh-7 cells. E-cadherin, α-SMA and vimentin played important roles in EMT process (40). Huang K et al has revealed that activation of TGF-β signaling could enhance the EMT process (41). Our results were consistent to these findings, suggesting that TGF-β signaling could promote EMT process during the fibrosis. Based on these data, LINC01234 has a potential ability for promoting liver cancer through activation of TGF-β1/EMT signaling.

Components of the PI3K/Akt pathway are targeted in more types of cancer than any other growth factor signaling pathway, and it is commonly activated as a cancer promoter (42). In our current research, LINC01234 knockdown significantly inactivated PI3K/Akt signaling. An earlier report similarly found that inactivation of PI3K/Akt signaling contributes to cancer cell apoptosis (43). Moreover, our findings suggested that knockdown of LINC01234 inactivated EMT process in liver cancer cells. Xiao L et al revealed that USP4 could activate PI3K/Akt to regulate the progression of peritoneal dialysis (44). Moreover, activation of PI3K/Akt could cause the upregulation of EMT process (45). Together with that report, our results suggested that USP4 promotes EMT process in liver cancer through activation of PI3K/Akt. Frankly speaking, in vivo study in this research only focused on the effect of LINC01234 on TGF-β signaling so far. Thus, we will investigate the effect of LINC01234 on PI3K/Akt signaling in vivo in a future study.

To sum up, LINC01234 was upregulated in liver cancer. In addition, LINC01234 knockdown could inhibit the growth, migration and invasion of liver cancer cells. LINC01234 mediated the tumorigenesis of liver cancer through mediation of miR-513a-5p/USP4 axis, which may act as a key biomarker for diagnosis and treatment of liver cancer.

Declarations

Conflicts of interests

These authors declared no competing interests in this study.

Acknowledgement

Not applicable

Author contribution

Wen Xu, Kesang Li, Changfeng Song, Xiaotong Wang, Wanli Deng, Junqing Wang and Jianwen Liu conceived and supervised the study; Yueqi Li, Xue Bai, Xin Liang and Jianwen Liu designed experiments. All authors reviewed the results and approved the final version of the manuscript.

Data availability

The data set supporting the results of this article are included within the article

References

1. Zhang H, Zhuo C, Zhou D, Zhang M, Zhang F, Chen M, et al. Small Nucleolar RNA Host Gene 1 (SNHG1) and Chromosome 2 Open Reading Frame 48 (C2orf48) as Potential Prognostic Signatures for Liver Cancer by Constructing Regulatory Networks. Med Sci Monit. 2020;26:e920482.

2. Ma X, Mo M, Tan HJJ, Tan C, Zeng X, Zhang G, et al. LINC02499, a novel liver-specific long non-coding RNA with potential diagnostic and prognostic value, inhibits hepatocellular carcinoma cell proliferation, migration, and invasion. Hepatol Res. 2020.
3. Dong H, Jian P, Yu M, Wang L. Silencing of long noncoding RNA LEF1-AS1 prevents the progression of hepatocellular carcinoma via the crosstalk with microRNA-136-5p/WNK1. J Cell Physiol. 2020.
4. Zhang H, Bao J, Zhao S, Huo Z, Li B. MicroRNA-490-3p suppresses hepatocellular carcinoma cell proliferation and migration by targeting the aurora kinase A gene (AURKA). Arch Med Sci. 2020;16:395-406.
5. Ba MC, Ba Z, Long H, Cui SZ, Gong YF, Yan ZF, et al. LncRNA AC093818.1 accelerates gastric cancer metastasis by epigenetically promoting PDK1 expression. Cell Death Dis. 2020;11:64.
6. Cao Y, Xiong JB, Zhang GY, Liu Y, Jie ZG, Li ZR. Long Noncoding RNA UCA1 Regulates PRL-3 Expression by Sponging MicroRNA-495 to Promote the Progression of Gastric Cancer. Mol Ther Nucleic Acids. 2020;19:853-64.
7. Jiao Y, Li Y, Jia B, Chen Q, Pan G, Hua F, et al. The prognostic value of lncRNA SNHG4 and its potential mechanism in liver cancer. Biosci Rep. 2020;40.
8. Guan YF, Huang QL, Ai YL, Chen QT, Zhao WX, Wang XM, et al. Nur77-activated lncRNA WFDC21P attenuates hepatocarcinogenesis via modulating glycolysis. Oncogene. 2020.
9. Tao Y, Wan X, Fan Q, Wang Y, Sun H, Ma L, et al. Long non-coding RNA OIP5-AS1 promotes the growth of gastric cancer through the miR-367-3p/HMGA2 axis. Dig Liver Dis. 2020.
10. Xu W, Yu S, Xiong J, Long J, Zheng Y, Sang X. CeRNA regulatory network-based analysis to study the roles of noncoding RNAs in the pathogenesis of intrahepatic cholangiocellular carcinoma. Aging (Albany NY). 2020;12:1047-86.
11. Ji H, Niu C, Zhan X, Xu J, Lian S, Xu B, et al. Identification, functional prediction, and key lncRNA verification of cold stress-related lncRNAs in rats liver. Sci Rep. 2020;10:521.
12. Ren F, Wang J, Aniagu S, Li J, Jiang Y, Chen T. Effects of Trichloroethylene on the Expression of Long Intergenic Noncoding RNAs in B6C3F1 Mouse Liver. Chem Res Toxicol. 2020.
13. Gupta M, Chandan K, Sarwat M. Role of miRNA and Long Non-Coding RNA in Hepatocellular Carcinoma. Curr Pharm Des. 2020.
14. Yu G, Li S, Liu P, Shi Y, Liu Y, Yang Z, et al. LncRNA TUG1 functions as a ceRNA for miR-6321 to promote endothelial progenitor cell migration and differentiation. Exp Cell Res. 2020;388:111839.
15. Zuo X, Chen Z, Gao W, Zhang Y, Wang J, Wang J, et al. M6A-mediated upregulation of LINC00958 increases lipogenesis and acts as a nanotherapeutic target in hepatocellular carcinoma. J Hematol Oncol. 2020;13:5.
16. Wang C, Jiang X, Li X, Song S, Meng Q, Wang L, et al. Long noncoding RNA HULC accelerates the growth of human liver cancer stem cells by upregulating CyclinD1 through miR675-PKM2 pathway via autophagy. Stem Cell Res Ther. 2020;11:8.

17. Jiang B, Yang B, Wang Q, Zheng X, Guo Y, Lu W. lncRNA PVT1 promotes hepatitis B viruspositive liver cancer progression by disturbing histone methylation on the cMyc promoter. Oncol Rep. 2020;43:718-26.
18. Yang JJ, Yang Y, Zhang C, Li J, Yang Y. Epigenetic silencing of LncRNA ANRIL enhances liver fibrosis and HSC activation through activating AMPK pathway. J Cell Mol Med. 2020;24:2677-87.
19. Qiu S, Chen G, Peng J, Liu J, Chen J, Wang J, et al. LncRNA EGOT decreases breast cancer cell viability and migration via inactivation of the Hedgehog pathway. FEBS Open Bio. 2020.
20. Xu Y, Xia X, Jiang Y, Wu D, Wang S, Fu S, et al. Down-regulated lncRNA AGAP2-AS1 contributes to pre-eclampsia as a competing endogenous RNA for JDP2 by impairing trophoblastic phenotype. J Cell Mol Med. 2020.
21. Zhang L, Zhang D, Qin ZY, Li J, Shen ZY. The role and possible mechanism of long noncoding RNA PVT1 in modulating 3T3-L1 preadipocyte proliferation and differentiation. IUBMB Life. 2020.
22. Liu C, Lu Z, Liu H, Zhuang S, Guo P. LncRNA XIST promotes the progression of laryngeal squamous cell carcinoma via sponging miR-125b-5p to modulate TRIB2. Biosci Rep. 2020.
23. Jin D, Song Y, Chen Y, Zhang P. Identification of Three lncRNAs as Potential Predictive Biomarkers of Lung Adenocarcinoma. Biomed Res Int. 2020;2020:7573689.
24. Wu M, Shen X, Tang Y, Zhou C, Li H, Luo X. Identification and validation of potential key long noncoding RNAs in sorafenib-resistant hepatocellular carcinoma cells. PeerJ. 2020;8:e8624.
25. Kaur H, Bhalla S, Kaur D, Raghava GP. CancerLivER: a database of liver cancer gene expression resources and biomarkers. Database (Oxford). 2020;2020.
26. Zhang GF, Qiu L, Yang SL, Wu JC, Liu TJ. Wnt/beta-catenin signaling as an emerging potential key pharmacological target in cholangiocarcinoma. Biosci Rep. 2020;40.
27. Yang L, Zhang L, Lu L, Wang Y. lncRNA UCA1 Increases Proliferation and Multidrug Resistance of Retinoblastoma Cells Through Downregulating miR-513a-5p. DNA Cell Biol. 2020;39:69-77.
28. Zhu Y, He D, Bo H, Liu Z, Xiao M, Xiang L, et al. The MRVI1-AS1/ATF3 signaling loop sensitizes nasopharyngeal cancer cells to paclitaxel by regulating the Hippo-TAZ pathway. Oncogene. 2019;38:6065-81.
29. Ma J, Han LN, Song JR, Bai XM, Wang JZ, Meng LF, et al. Long noncoding RNA LINC01234 silencing exerts an anti-oncogenic effect in esophageal cancer cells through microRNA-193a-5p-mediated CCNE1 downregulation. Cell Oncol (Dordr). 2020.
30. Liang Y, Song X, Li Y, Ma T, Su P, Guo R, et al. Targeting the circBMPR2/miR-553/USP4 Axis as a Potent Therapeutic Approach for Breast Cancer. Mol Ther Nucleic Acids. 2019;17:347-61.
31. Nguyen HH, Kim T, Nguyen T, Hahn MJ, Yun SI, Kim KK. A Selective Inhibitor of Ubiquitin-Specific Protease 4 Suppresses Colorectal Cancer Progression by Regulating beta-Catenin Signaling. Cell Physiol Biochem. 2019;53:157-71.
32. Geng N, Li Y, Zhang W, Wang F, Wang X, Jin Z, et al. A PAK5-DNPEP-USP4 axis dictates breast cancer growth and metastasis. Int J Cancer. 2020;146:1139-51.

33. Zhang J, Na S, Pan S, Long S, Xin Y, Jiang Q, et al. Inhibition of USP4 attenuates pathological scarring by downregulation of the TGFbeta/Smad signaling pathway. Mol Med Rep. 2019;20:1429-35.
34. Qiu C, Liu Y, Mei Y, Zou M, Zhao Z, Ye M, et al. Ubiquitin-speci fi c protease 4 promotes metastasis of hepatocellular carcinoma by increasing TGF-beta signaling-induced epithelial-mesenchymal transition. Aging (Albany NY). 2018;10:2783-99.
35. Heo MJ, Kim YM, Koo JH, Yang YM, An J, Lee SK, et al. microRNA-148a dysregulation discriminates poor prognosis of hepatocellular carcinoma in association with USP4 overexpression. Oncotarget. 2014;5:2792-806.
36. Shi X, Shao X, Liu B, Lv M, Pandey P, Guo C, et al. Genome-wide screening of functional long noncoding RNAs in the epicardial adipose tissues of atrial fibrillation. Biochim Biophys Acta Mol Basis Dis. 2020:165757.
37. Wang JN, Yang Q, Yang C, Cai YT, Xing T, Gao L, et al. Smad3 promotes AKI sensitivity in diabetic mice via interaction with p53 and induction of NOX4-dependent ROS production. Redox Biol. 2020;32:101479.
38. Nyati S, Gregg BS, Xu J, Young G, Kimmel L, Nyati MK, et al. TGFBR2 mediated phosphorylation of BUB1 at Ser-318 is required for transforming growth factor-beta signaling. Neoplasia. 2020;22:163-78.
39. Sakamoto R, Kajihara I, Miyauchi H, Maeda-Otsuka S, Yamada-Kanazawa S, Sawamura S, et al. Inhibition of endoglin exerts anti-tumor effects through the regulation of non-Smad TGF-beta signaling in angiosarcoma. J Invest Dermatol. 2020.
40. He J, Jiang YL, Wang Y, Tian XJ, Sun SR. Micro-vesicles from mesenchymal stem cells over-expressing miR-34a inhibit transforming growth factor-beta1-induced epithelial-mesenchymal transition in renal tubular epithelial cells in vitro. Chin Med J (Engl). 2020.
41. Huang K, Gao N, Bian D, Zhai Q, Yang P, Li M, et al. Correlation between FAK and EGF-Induced EMT in Colorectal Cancer Cells. J Oncol. 2020;2020:5428920.
42. Zhang M, Wang X, Liu M, Liu D, Pan J, Tian J, et al. Inhibition of PHLPP1 ameliorates cardiac dysfunction via activation of the PI3K/Akt/mTOR signalling pathway in diabetic cardiomyopathy. J Cell Mol Med. 2020.
43. Pan S, Ren F, Li L, Liu D, Li Y, Wang A, et al. MiR-328-3p inhibits cell proliferation and metastasis in colorectal cancer by targeting Girdin and inhibiting the PI3K/Akt signaling pathway. Exp Cell Res. 2020:111939.
44. Xiao L, Peng X, Liu F, Tang C, Hu C, Xu X, et al. AKT regulation of mesothelial-to-mesenchymal transition in peritoneal dialysis is modulated by Smurf2 and deubiquitinating enzyme USP4. BMC Cell Biol. 2015;16:7.
45. Peng Y, Li F, Zhang P, Wang X, Shen Y, Feng Y, et al. IGF-1 promotes multiple myeloma progression through PI3K/Akt-mediated epithelial-mesenchymal transition. Life Sci. 2020:117503.

Figures

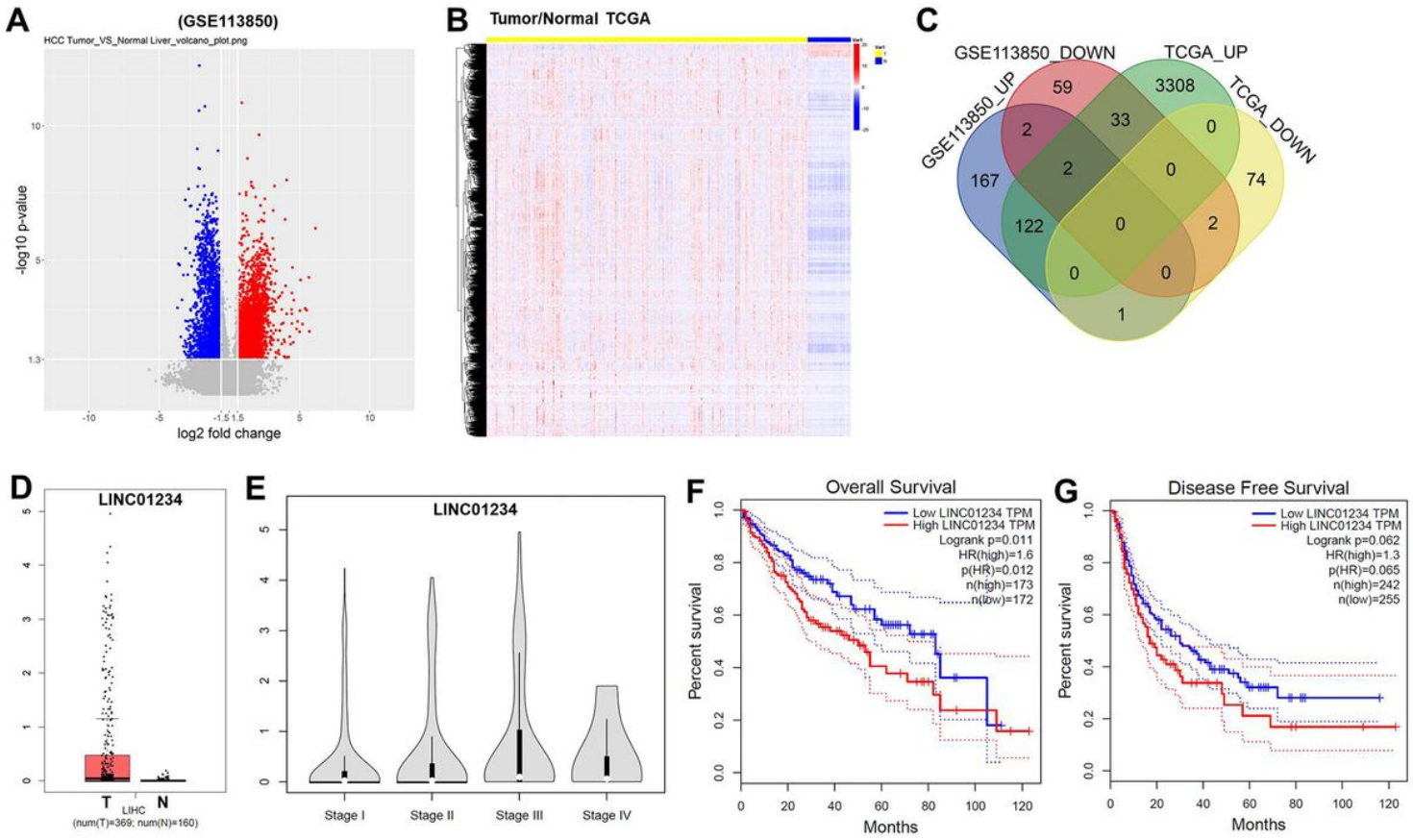

Figure 1

Differentially expressed lncRNAs in liver cancer. (A) Volcano plots illustrating the lncRNAs differentially expressed in hepatic carcinoma detected in the GSE113850 dataset. Red indicates a higher expression level, while blue indicates a lower expression level. (B) Differentially expressed lncRNAs among normal and liver cancer tissues were presented by TCGA. (C) Venn diagram showing the overlap among the differentially expressed lncRNAs in the GSE113850 dataset. (D) The expression of LINC01234 in normal or tumor tissues was detected by TCGA. (E) The expression of LINC01234 in different stages of liver cancer tissues was investigated by TCGA. (F, G) Overall and disease free survival of hepatic carcinoma were analyzed by TCGA.

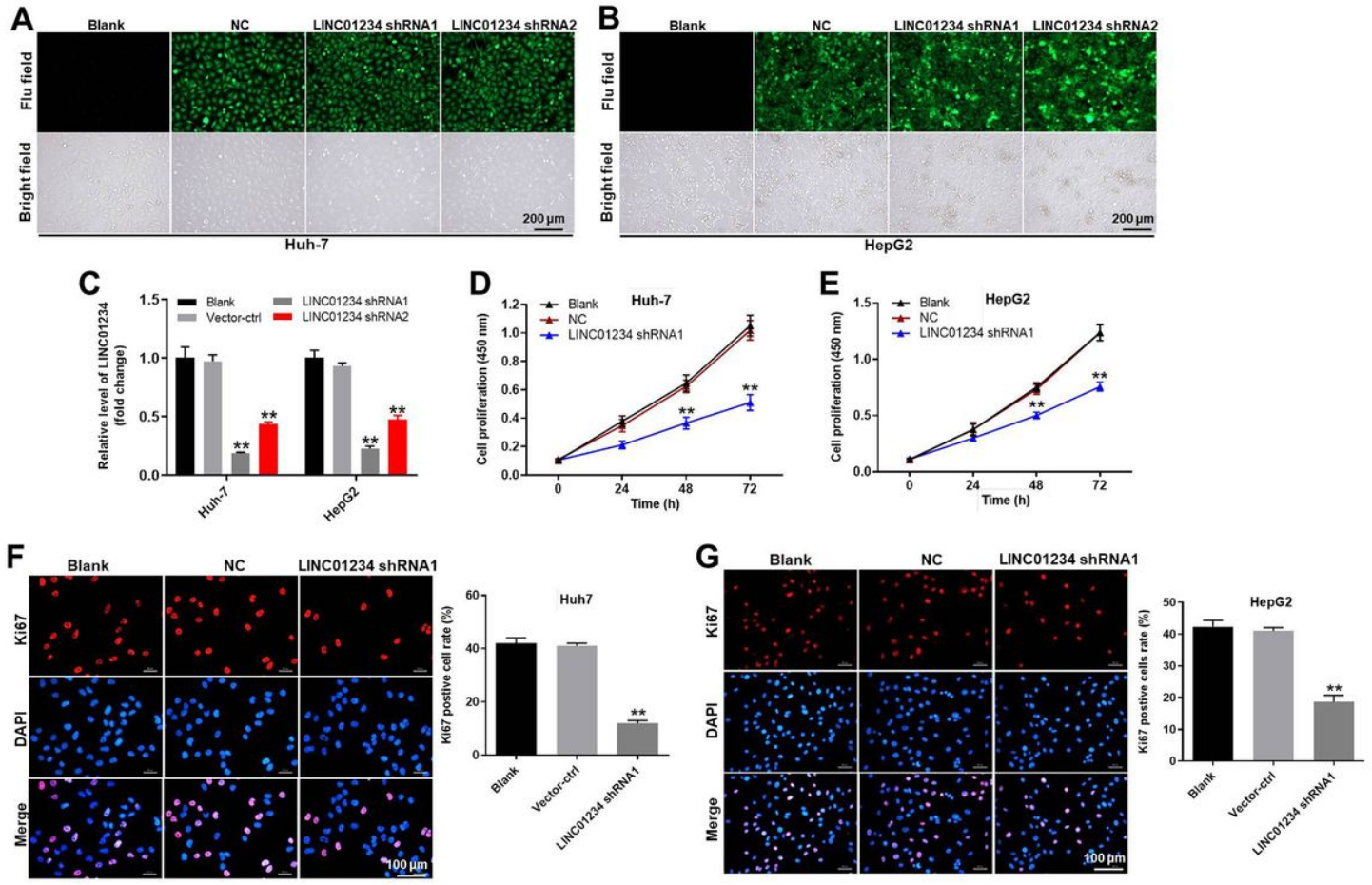

Figure 2

LINC01234 silencing significantly decreased the proliferation of liver cancer cells. Huh-7 cells were transfected with LINC01234 shRNA1/shRNA2 for 24 h. Then, (A, B) the efficiency of cell transfection was detected by green fluorescence staining. (C) The expression of LINC01234 in liver cancer cells was detected by q-PCR. The proliferation of (D) Huh-7 or (E) HepG2 cells was detected by CCK-8 assay. (F, G) Ki-67 staining was performed to test the proliferation of Huh-7 and HepG2 cells. Red indicates the Ki-67 staining. Blue indicates DAPI staining. **P< 0.01 compared to control.

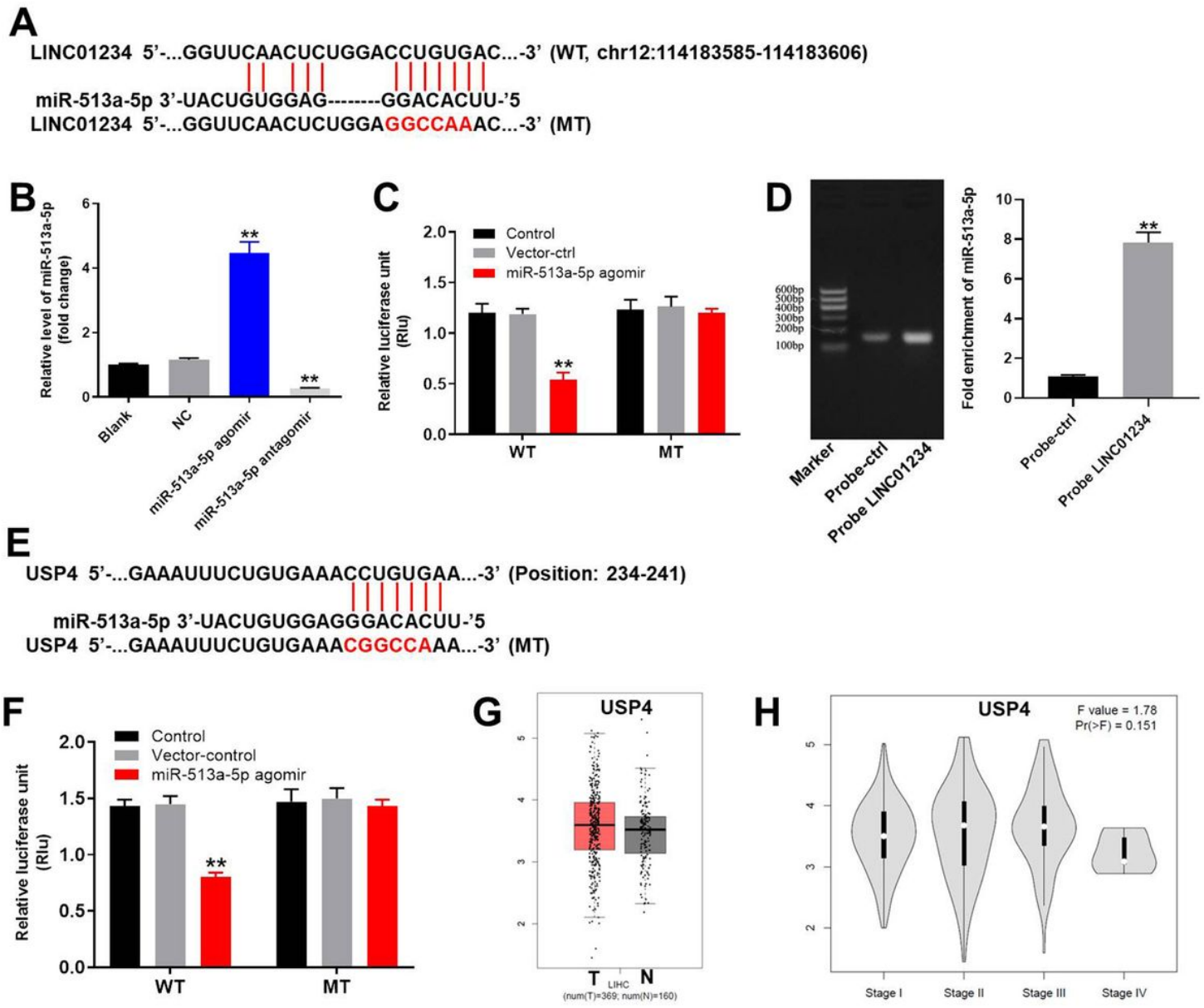

Figure 3

LINC01234 sponged miR-513a-5p. (A) Gene structure of LINC01234 indicating the predicted miR-513a-5p binding site in its 3'UTR. (B) Huh-7 cells were transfected with miR-513a-5p agomir/antagomir for 24 h. Then, cell transfection was verified by q-PCR. (C) The luciferase activity in Huh-7 cells after co-transfecting a plasmid encoding the wild-type (WT) or mutant (MT) LINC01234 3'-UTR and miR-513a-5p. (D) Co-localization of LINC01234 and miR-513a-5p detected using RNA pull-down. (E) Gene structure of USP4 indicating the predicted miR-513a-5p binding site in its 3'UTR. (F) The luciferase activity in Huh-7 cells after co-transfecting a plasmid encoding the wild-type (WT) or mutant (MT) USP4 3'-UTR and miR-513a-5p. (G) The expression of USP4 in normal or tumor tissues was detected by TCGA. (H) The expression of USP4 in different stages of hepatic carcinoma was detected by TCGA. **P< 0.01 compared to control.

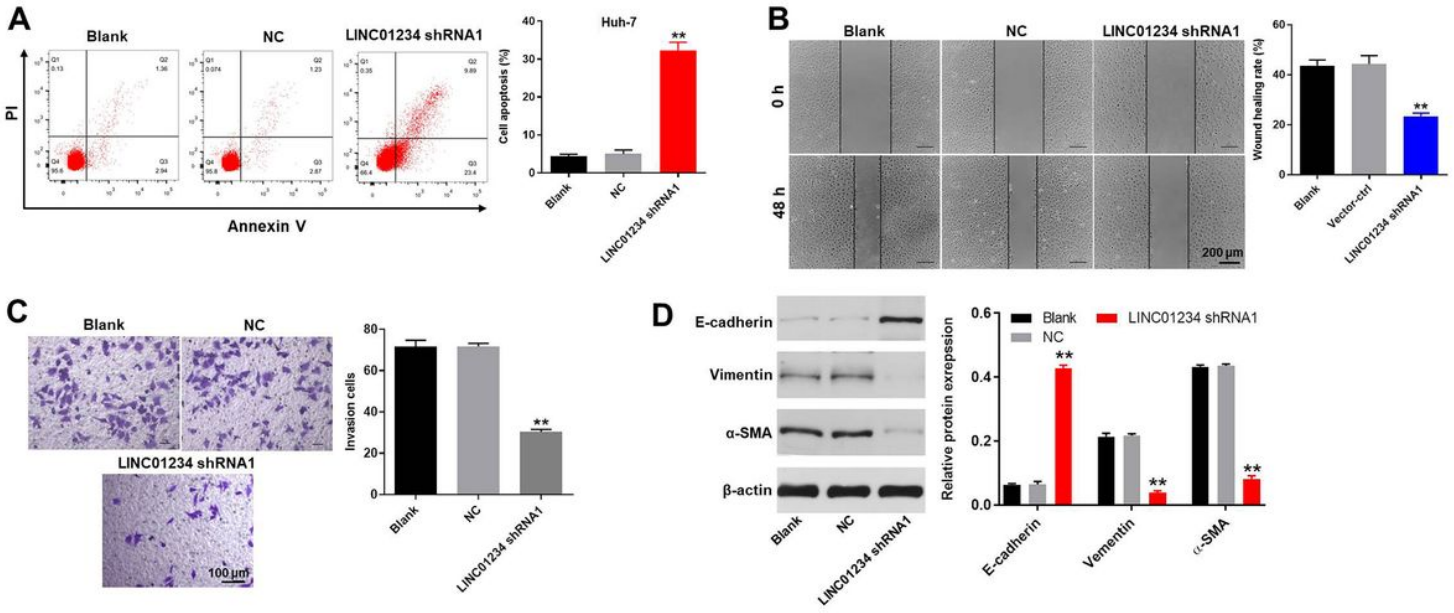

Figure 4

Knockdown of LINC01234 significantly suppressed the progression of hepatic carcinoma in vitro. (A) The apoptotic Huh-7 cells were examined by flow cytometry. (B) Cell migration was measured by wound healing assay. (C) Cell invasion was detected by transwell assay. (D) The protein expressions of E-cadherin, vimentin and α-SMA in Huh-7 cells were detected by western blot. The relative protein expressions were quantified by normalizing to β-actin. **P< 0.01 compared to control.

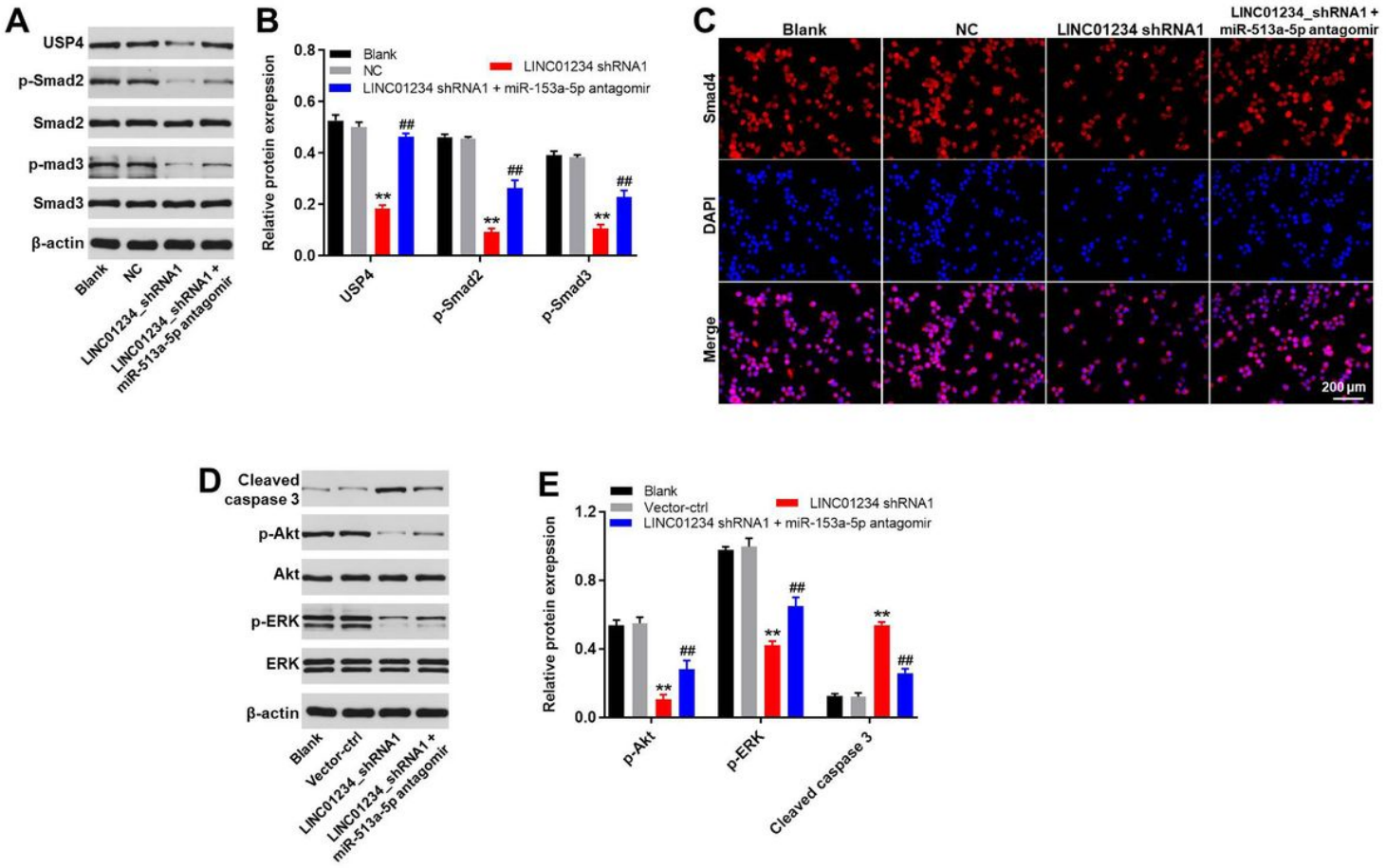

Figure 5

Downregulation of LINC01234 notably inhibited the tumorigenesis of hepatic carcinoma via mediation of miR-513a-5p/USP4/TGF-β1 axis. (A) The protein expressions of USP4, Smad2, Smad3, p-Smad2 and p-Smad3 in Huh-7 cells were detected by western blot. (B) The relative protein expressions were quantified by normalizing to β-actin. (C) The expression of Smad4 was detected by immunofluorescence staining. Red indicates Smad4 fluorescence. Blue indicates DAPI fluorescence. (D) The protein expressions of Akt, p-Akt, cleaved caspase 3, ERK and p-ERK in Huh-7 cells were measured by western blot. (E) The relative protein expressions were quantified by normalizing to β-actin. **P< 0.01 compared to control. ##P< 0.01 compared to LINC01234 shRNA1.

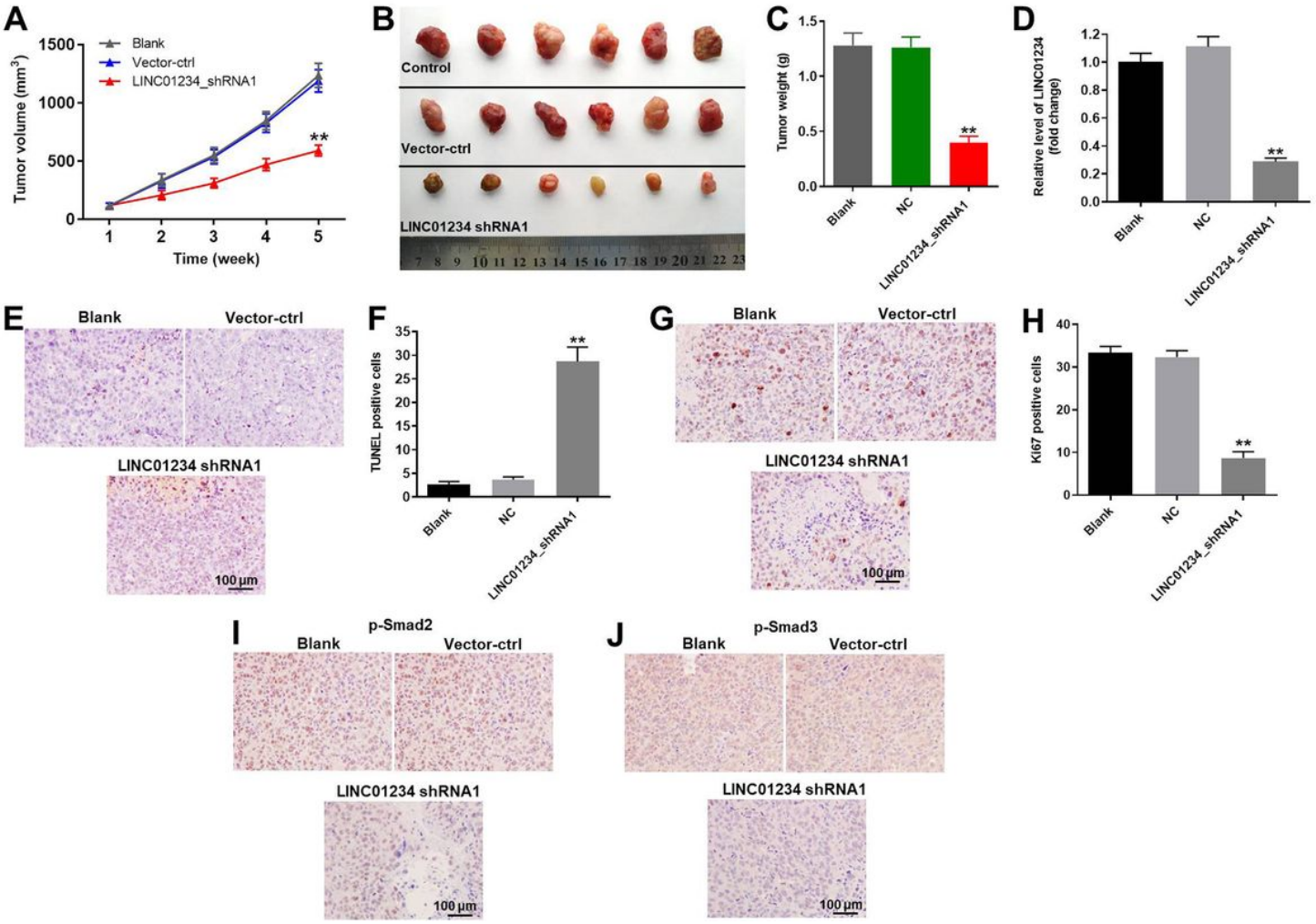

Figure 6

Knockdown of LINC01234 notably attenuated the symptom of hepatic carcinoma in vivo through suppression of TGF-β signaling. Mice were subcutaneously injected Huh-7 cells transfected with vector-control or LINC01234 shRNA1 or left untreated (Blank), after which tumors were allowed to grow for 5 weeks. (A) Volumes of tumors collected at the indicated times after transplantation. At the end of study, (B) tumor tissues were collected and imaged. (C) Tumors of each mouse were weighted. (D) The expression of LINC01234 in tumor tissues of mice was detected by q-PCR. (E, F) The apoptotic cells in tumor tissues of mice were detected by TUNEL staining. (G, H) Ki-67 staining was performed to test the proliferation of liver cancer cells. (I, J) The expression of p-Smad2 and p-Smad3 in tumor tissues of mice were detected by IHC staining. **P< 0.01 compared to control.